

Mean monthly radiation surfaces for Australia at 1 arc-second resolution

J.M. Austin^a, J.C. Gallant^a and T. Van Niel^b

^a CSIRO Land and Water, Black Mountain Laboratories, Canberra ACT 2600, Australia

^b CSIRO Land and Water, Floreat WA, Australia

Email: jenet.austin@csiro.au

Abstract: Solar radiation data are useful for many purposes including ecological and hydrological modelling and for assessing available solar energy. Using the new national 1 arc-second DEM, the SRAD model, and national climate, albedo, and vegetation cover data, we have created mean monthly radiation surfaces for Australia: total shortwave on a sloping surface (SWS), total shortwave on a horizontal surface (SWH), the ratio of sloping to horizontal shortwave (SWR), incoming atmospheric longwave (LIN), outgoing surface longwave (LOUT), net longwave (LNET), and net radiation (RNET). The output datasets will be available through the TERN Data Discovery Portal (<http://portal.tern.org.au>) and the CSIRO Data Access Portal (<http://data.csiro.au/dap>).

Modelling solar radiation using DEMs can be undertaken with varying degrees of complexity and parameterisations. Calculating the position of the sun and length of the day are relatively straightforward but the effects of clouds, scattering and absorption in the atmosphere, topographic shadowing, and reflection from sloping surfaces make precise calculation of radiation at the surface exceedingly difficult. SRAD models the solar radiation incident upon a sloping surface accounting for the solar geometry on a given day, the surface orientation, shadowing by surrounding terrain and the transmittance of the atmosphere and clouds, and calculates incoming and outgoing longwave radiation based on air and surface temperatures and emissivities. The model uses elevation, slope and aspect, and 12 mean monthly surfaces for albedo, fractional vegetation cover, 9 am and 3 pm cloud cover, minimum and maximum air temperature, and 9 am and 3 pm vapour pressure. The relationship between cloud fraction and sunshine fraction was modelled by linear regression with observed cloud and sunshine from the BoM, while observed cloud fraction, sunshine fraction and incoming shortwave radiation data were used to determine the clear sky and cloud transmittance parameters.

Figure 1 shows examples of the SRAD SWS outputs for January and July in south-western Tasmania. A preliminary comparison of the SWH outputs for January and July with observed radiation data for 6 stations shows differences of less than 2% for 7 of the 12 comparisons and differences of 5% to 15% in the other 5. The causes of these differences are not yet known but differences in the period of record for parameterisation and validation is one possibility. Expanding the validation to include 12 months and 37 BoM stations should help to make this clearer.

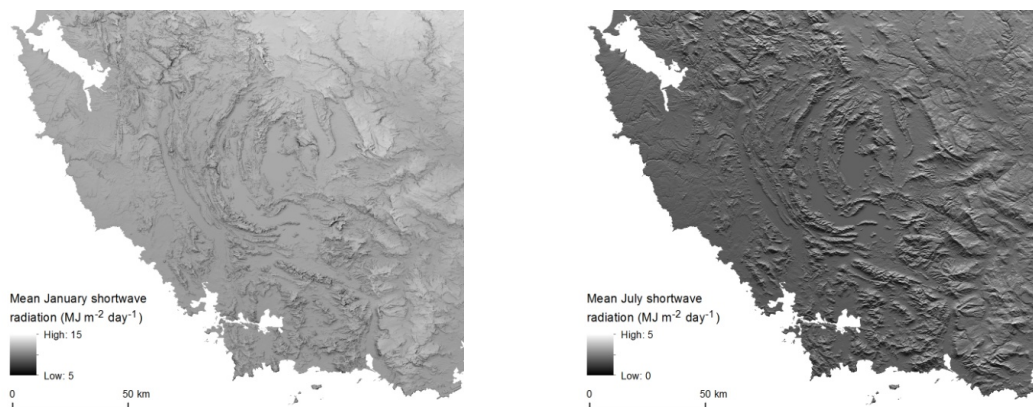


Figure 1. Modelled mean monthly total shortwave radiation on a sloping surface for January (left) and July (right) in south-western Tasmania. Note: these radiation values are from an earlier model run with less rigorous parameterization, and are an underestimate compared to observed values.

Keywords: Solar radiation, Climate surfaces, Digital elevation model

1. INTRODUCTION

Solar radiation data are useful for many purposes including ecological and hydrological modelling and for assessing available solar energy (Liu *et al.*, 2012). The Terrestrial Ecosystem Research Network (TERN) Soils Facility, for example, requires mean monthly radiation estimates for Australia for use in digital soil mapping.

The recent production of the Shuttle Radar Topographic Mission (SRTM) derived 1 arc-second resolution digital elevation model (DEM) for Australia (Gallant *et al.*, 2011) has created an opportunity to model solar radiation across the continent with fine scale terrain data as inputs. Other sources of radiation data, such as the Bureau of Meteorology (BoM) daily global solar exposure product (<http://www.bom.gov.au/climate/austmaps/about-solar-maps.shtml>) and previous national long-term radiation estimates (e.g. Hutchinson *et al.*, 1984), lack the fine-scale terrain effects that are critical to differentiating between exposed and protected sites and predicting the ecological and hydrological effects of those patterns.

There are many approaches to modelling solar radiation using DEMs, with varying degrees of complexity and parameterisations. Calculating the position of the sun and length of the day are relatively straightforward but the effects of clouds, scattering and absorption in the atmosphere, topographic shadowing, and reflection from sloping surfaces make precise calculation of radiation at the surface exceedingly difficult. Consequently a number of simplifications and empirical approximations are used. Ruiz-Arias *et al.* (2009) compare four approaches, including the SRAD model used here. SRAD has moderate complexity but can be parameterised using available measurements of radiation and sunshine hours.

2. SRAD MODEL

For this work we used the SRAD solar radiation model. SRAD is documented in Moore *et al.* (1993) and Wilson and Gallant (2000), and an example of its use is described in Gallant (1997). The SRAD model calculates incoming shortwave and both incoming and outgoing longwave radiation for every cell in a grid DEM for a single day (or average values for multiple days at defined intervals). The DEM is used to calculate the angle to the horizon in 16 directions, the orientation of the land surface and the proportion of sky and ground visible for every DEM cell. The position of the sun in the sky for the modelled day is calculated at 12 minute intervals from sunrise to sunset and the direct and diffuse components of incoming shortwave radiation are accumulated for each interval. Atmospheric effects are parameterised by clear-sky transmittance, cloud transmittance and the fraction of the day that is free of clouds (sunshine fraction). The shortwave radiation is used together with vegetation cover information to modulate a supplied surface temperature layer, to apply the fine-scale terrain effects to the broad scale temperature information, and the surface temperature is used to compute outgoing longwave radiation. Incoming longwave is calculated from average air temperature and an emissivity derived from vapour pressure and cloudiness; both incoming and outgoing longwave radiation are calculated for the full 24 hour period. Daily net radiation is computed from the shortwave and longwave components and surface albedo. All the input parameters are specified as mean monthly values.

The original SRAD model was written in FORTRAN, and the version used for this study was implemented in IDL (Interactive Data Language). Compared to previous versions, this version has been modified to accept fractional vegetation cover, cloud fraction and albedo as surfaces for each month rather than single value parameters. It also uses a morning and afternoon sunshine fraction, rather than a single value for the whole day. Additionally, the slope, aspect and horizon angle calculations, which depend only on the DEM, were separated from the radiation calculations so they could be calculated once rather than be re-calculated for each monthly analysis. This version of the model requires the following input surfaces:

- Elevation
- Slope
- Aspect
- Mean monthly surface albedo
- Mean monthly fractional vegetation cover (used to calculate leaf area index)
- Mean monthly cloud fraction at 9 am and 3 pm (used to calculate morning and afternoon sunshine fraction)
- Mean monthly minimum and maximum air temperature (used to calculate mean surface temperature)
- Mean monthly vapour pressure (used to derive atmospheric emissivity)

The radiation surfaces produced by SRAD are total shortwave on a horizontal surface, total shortwave on a sloping surface, the ratio of sloping to horizontal shortwave, incoming atmospheric longwave, outgoing surface longwave, net longwave, and net radiation. A number of other components are calculated internally, such as horizon angles, diffuse radiation and direct radiation, but are not reported in the current implementation.

3. METHODS

3.1. Input Datasets

Terrain Data

The input elevation surface was the 1 arc-second resolution SRTM-derived smoothed DEM (DEM-S) for Australia (Gallant *et al.*, 2011). Aspect and slope were calculated from the DEM-S using the finite difference method (Gallant and Wilson, 2000). The different spacing in the E-W and N-S directions due to the geographic projection of the data was accounted for by using the actual spacing in metres of the grid points calculated from the latitude. The SRAD model calculates horizon angles using the profile-based method of Dozier *et al.* (1981).

Temporal Data

Cloud fraction surfaces were calculated from spatially interpolated cloud cover fraction observations at 9 am and 3 pm using data from 165 BoM stations over the period 1981 to 2006 (Jovanovic *et al.*, 2011). The two cloud fractions were computed at 0.05° (approximately 5 km) spatial resolution.

Albedo was calculated from monthly values derived from AVHRR over the period 1981 to 2006 at 0.05° spatial resolution (Donohue *et al.*, 2010a; Donohue *et al.*, 2010b).

Monthly minimum and maximum air temperature and 9 am and 3 pm vapour pressure surfaces at 0.05° spatial resolution were obtained for the period 1981 to 2006 (BoM, 2011; Jones *et al.*, 2009) and long-term averages for each month were calculated. Surface temperature was estimated as the average of maximum and minimum air temperature. The mean vapour pressure was used to derive atmospheric emissivity.

Leaf area index (LAI) at 0.05° spatial resolution was derived from AVHRR-based fractional cover (fcov) surfaces (Donohue *et al.*, 2008; Donohue *et al.*, 2010b) using the relationship:

$$\text{LAI} = -2 \ln(1 - \text{fcov}) \quad (1)$$

All the temporal input datasets were long-term monthly averages for the period 1981 to 2006.

Observed Data

Observed half hourly radiation data (MJ m⁻²), daily sunshine hours, and daily 9 am and 3 pm cloud cover (oktas) were obtained from the BoM for all available stations; the record lengths vary between stations. The daily sunshine hours, half hourly radiation and cloud cover data were used in the parameterization of the model, and the half hourly radiation data were aggregated to long term monthly means for validation of the model outputs.

3.2. Parameterization

Long-term monthly mean cloud fractions (*cf*) were converted to monthly mean sunshine fractions (*sf*) using the linear function:

$$sf = 1.084 - 0.870 * cf \quad (2)$$

This function was obtained by least-squares fitting of monthly *sf* (observed sunshine hours divided by calculated day length) to monthly *cf* (average of 9am and 3pm cloud cover in oktas divided by 8). The monthly values were aggregated from daily records from 1981 through 2006, and the monthly means were only included in the analysis if they comprised more than 100 daily observations over that 26-year period. Figure 2 shows the *sf* and *cf* values and the fitted line, which has an *R*² of 0.80.

In this version of the SRAD model, Equation 2 was used to calculate morning sunshine fraction (sunrise to midday) from 9 am cloud fraction surfaces, and afternoon sunshine fraction (midday to sunset) from 3 pm cloud fraction surfaces.

Atmospheric transmittance and cloud transmittance were derived from the coefficients in the modified Angstrom equation:

$$\frac{Q}{H_0} = a + b sf \tag{3}$$

Q is daily global radiation obtained from BoM data, H_0 is extra-terrestrial radiation (the radiation on a horizontal surface if there was no atmosphere) calculated using the equations from Iqbal (1983) and sf is sunshine fraction as in (2). Clear sky transmittance is $a + b$ and cloud transmittance is $a/(a + b)$. Figure 3 shows a plot of sf versus Q/H_0 values for all months. The R^2 values for the monthly relationships are all higher than the annual aggregate R^2 of 0.924 shown in Figure 3. Table 1 lists the monthly clear sky and cloud transmittance values used in the model and the R^2 values for the monthly functions; the number of values changes due to the different record lengths and missing data. The circumsolar coefficient was fixed both spatially and temporally at 0.25.

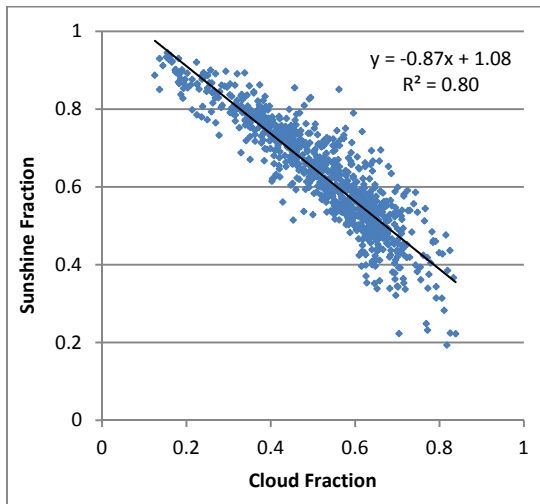


Figure 2. Plot of monthly sunshine fraction versus cloud fraction. The black line is the linear function fitted to the data.

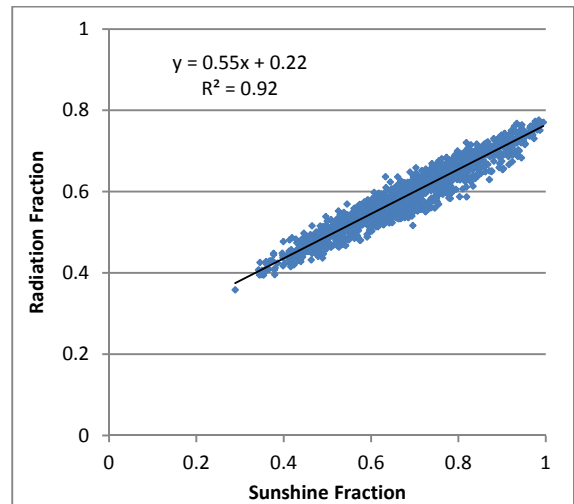


Figure 3. Monthly radiation fraction Q/H_0 versus sunshine fraction for all months. The black line is the linear function fitted to all points. The relationships for individual months, as used in the model, vary from this overall relationship and have less scatter

Table 1. Clear sky and cloud transmittance values derived from observed monthly cloud fraction, sunshine fraction and shortwave radiation ($\text{MJ m}^{-2} \text{d}^{-1}$), and the number of monthly input values and the R^2 for the relationship.

Month	Clear sky transmittance	Cloud transmittance	Number of values	R^2
1	0.790	0.253	109	0.974
2	0.790	0.233	111	0.986
3	0.789	0.241	111	0.981
4	0.762	0.243	111	0.985
5	0.757	0.262	110	0.988
6	0.749	0.297	112	0.985
7	0.753	0.290	108	0.986
8	0.752	0.293	108	0.982
9	0.757	0.325	111	0.974
10	0.763	0.283	113	0.956
11	0.756	0.329	113	0.953
12	0.779	0.292	107	0.956

3.3. Processing

Atmospheric and land surface parameters at coarser resolutions than the 1 arc-second DEM were resampled to the DEM resolution using bilinear interpolation. The radiation calculations were performed on $1^\circ \times 1^\circ$ tiles, with 5 km overlaps to ensure correct handling of shadowing at tile edges. Calculation of the global horizon surface once for each $1^\circ \times 1^\circ$ tile saved a substantial amount of time during processing.

The SRTM DEM for Australia consists of 813 $1^\circ \times 1^\circ$ tiles. Running the model on each tile required 10 GB of memory and 5 hours of processing time per month. Using a CSIRO shared-memory super computer with help from the CSIRO Advanced Scientific Computing team, up to 200 tiles were run concurrently. Production of the complete SRAD dataset for Australia, i.e. 12 monthly surfaces for each of the 7 SRAD radiation outputs, took approximately 2 months of elapsed time. Without parallel processing it would have taken over 5 years to generate the SRAD outputs for Australia at this resolution.

4. RESULTS

The outputs from the SRAD model are long-term mean radiation surfaces for each month with units of $\text{MJ m}^{-2} \text{d}^{-1}$. The output surfaces cover the same area as the source DEM-S, which is virtually all of continental Australia and near coastal islands. Some DEM tiles containing mainland or pieces of islands were not supplied at 1 arc-second resolution and are therefore missing. Figure 1 shows the total shortwave on a sloping surface outputs for January and July in south-western Tasmania.

The output datasets will be publicly available through the TERN Data Discovery Portal (<http://portal.tern.org.au>) and the CSIRO Data Access Portal (<http://data.csiro.au/dap>). The data will be available as continental mosaics and as tiles, at resolutions of 1, 3 and 9 arc-seconds. The 3 and 9 arc-second resolution surfaces were produced by resampling the 1 arc-second data and taking the average value.

4.1. Preliminary validation

Of the SRAD model outputs, the total shortwave on a horizontal surface (SRAD SWH) was directly comparable with the BoM observed global solar exposure (BoM global), the latter defined as the total amount of solar energy falling on a horizontal surface of unit area. BoM half hourly global solar exposure observations were aggregated to long term monthly means for the period 1981 to 2006; there are 22 stations across Australia with radiation records during that period. For the aggregation, only days with the full set of 48 half hourly observations were included in the long term mean monthly calculations.

Table 2. Comparison of SRAD total shortwave radiation on a horizontal surface with BoM global solar exposure measurements for selected meteorological stations across Australia.

BoM Station ID	Station Name	Lat (deg)	Long (deg)	January				July			
				SRAD SWH ($\text{MJ m}^{-2} \text{d}^{-1}$)	BoM global	SRAD minus Obs	Diff %	SRAD SWH ($\text{MJ m}^{-2} \text{d}^{-1}$)	BoM global	SRAD minus Obs	Diff %
8051	Geraldton Airport Comparison	-28.80	114.70	30.54	28.97	1.56	5.4	10.98	12.17	-1.19	-9.8
14015	Darwin Airport	-12.42	130.89	18.57	18.69	-0.12	-0.7	19.51	19.80	-0.29	-1.5
15590	Alice Springs Airport	-23.80	133.89	29.08	28.75	0.33	1.1	15.99	16.01	-0.02	-0.1
39083	Rockhampton Aero	-23.38	150.48	24.44	24.57	-0.13	-0.5	13.66	15.01	-1.34	-9.0
70014	Canberra Airport Comparison	-35.30	149.20	27.44	27.03	0.40	1.5	8.76	8.89	-0.14	-1.5
91148	Cape Grim Radiation	-40.68	144.69	22.36	24.42	-2.05	-8.4	5.22	6.14	-0.92	-15.0

Table 2 compares the SRAD SWH estimates with the BoM global observed values for 6 meteorological stations across Australia for the months of January and July; the stations were selected to cover a range of latitudes and climates. The SRAD SWH estimates for Darwin, Alice Springs and Canberra are very similar to the BoM global values for both months, whereas for Geraldton, Rockhampton and Cape Grim there is a 9-15 % underestimation for July compared to the BoM observations. The source of these differences is being investigated and other stations and months have not yet been examined.

5. DISCUSSION AND CONCLUSIONS

Incoming short-wave and long-wave radiation were calculated from solar geometry and atmospheric parameters and are subject to errors primarily from the atmospheric parameters. Outgoing long-wave radiation was calculated from surface temperature which was partly parameterised and partly driven by incoming radiation, surface albedo, and vegetation cover; this term is subject to larger uncertainty than the incoming radiation terms. Net radiation is the difference of incoming and outgoing terms and is therefore also subject to substantial uncertainty.

It is possible that there are spatial patterns in the relationship between sunshine fraction and cloud fraction – due to differences in cloud types, for example – that would account for some of the scatter in Figure 2, and this will be the subject of further investigation. The very high R^2 values for the sf /transmittance functions (Table 1) mean that there is very little room for spatial variations to play a significant role.

The observed radiation data used for the validation in Table 2 do not cover the same time period (1981-2006) as the data used to parameterise the SRAD model. For 5 of the 6 stations the observations were available only for the period 1999-2006, with Canberra the exception (1983-1994). Long-term changes in cloud frequency or transmittance could account for the difference between these observations and the SRAD predictions. Jovanovic *et al.* (2011) found various trends in total cloud amount over the period 1957-2007: Marrawah, near Cape Grim, (records start 1971) has no trend, Rockhampton (start 1957) has -0.011 oktas/decade, Geraldton (start 1955) has -0.075 oktas/decade and Canberra Airport (start 1955) has a strong negative trend of -0.095 oktas/decade. Declining cloud cover over the period 1981-2006 imply increased radiation in the period when the observations were taken (1999-2006) compared to the whole period, leading to a systematic under-prediction by the model. The reported trends in cloud cover could explain the difference between observed and modelled July radiation for Geraldton, but the relatively large under-predictions of radiation for Cape Grim are not matched by a cloudiness trend at the nearby Marrawah station. A closer examination of the cloud fraction records for all stations for the period of the radiation observations should reveal whether changes in cloud cover can explain the differences between predictions and observations.

Several approaches could be explored for improving the parameterisation to address the errors in predicted radiation for some sites in Table 2. Some options are:

- Examine the patterns in the residuals from the sf/cf regression and determine whether spatial and/or temporal variations in that relationship are necessary.
- Derive cloud occurrence from satellite imagery rather than spatially interpolate observed cloud cover fractions. This has the potential to improve the spatial resolution of the cloud information, although the length of the satellite time series may be an issue.
- Explore whether a non-linear least-squares regression is more appropriate for the sf/cf relationship.

Many components of SRAD could be improved and some of the compromises between accuracy and practicality reflect the available data when the model was first developed in the early 1990s. Satellite observations now provide routine and spatially detailed measurement of some of the parameters currently estimated from ground observations. The MODIS BRDF/Albedo products, for example, provide albedo for both direct and diffuse illumination (black-sky and white-sky albedo; Schaaf *et al.*, 2002) and cloud cover could also be derived with much greater spatial detail using MODIS imagery.

A more thorough validation of the SRAD results would include measured radiation on sloping surfaces of various inclinations in different climates. To the authors' knowledge there are no such measurements available in Australia. There may be value in establishing radiation monitoring stations in complex landscapes to provide high quality data for testing and improving models such as SRAD.

ACKNOWLEDGMENTS

This work has been funded by the Terrestrial Ecosystem Research Network Soils Facility. We gratefully acknowledge the help and advice given by Aaron McDonough of the CSIRO Advanced Scientific Computing team.

REFERENCES

- Bureau of Meteorology (2011). Australian Water Availability Project, <http://www.bom.gov.au/jsp/awap>, accessed 2nd December 2011.
- Donohue R.J., T.R. McVicar, and M.L. Roderick (2010a). Assessing the ability of potential evaporation formulations to capture the dynamics in evaporative demand within a changing climate. *Journal of Hydrology*, 386, 186-197.
- Donohue, R.J., T.R. McVicar, L. Lingtao, and M.L. Roderick (2010b). A data resource for analysing dynamics in Australian ecohydrological conditions. *Austral Ecology*, 35, 593–594.
- Donohue, R.J., M.L. Roderick and T.R. McVicar (2008). Deriving consistent long-term vegetation information from AVHRR reflectance data using a cover-triangle-based framework. *Remote Sensing of Environment*, 112(6), 2938-2949.
- Gallant, J.C. (1997). Modelling solar radiation in the forests of Southeastern Australia. *International Congress on Modelling and Simulation (MODSIM97)*. 8-11 December 1997, Hobart, Australia.
- Gallant, J.C., T.I. Dowling, A.M. Read, N. Wilson, P.K. Tickle, and C. Inskeep (2011). 1 second SRTM-derived Digital Elevation Models User Guide. Geoscience Australia www.ga.gov.au/topographic-mapping/digital-elevation-data.html.
- Hutchinson, M.F., T.H. Booth, J.P. McMahon, and H.A. Nix (1984). Estimating monthly mean values of daily total solar radiation for Australia. *Solar Energy*, 32(2), 277-290.
- Iqbal, M. (1983). *An Introduction to Solar Radiation*. Academic Press, Toronto.
- Jones, D.A., W. Wang, and R. Fawcett (2009). High-quality spatial climate data-sets for Australia. *Australian Meteorological and Oceanographic Journal*, 58, 233-248.
- Jovanovic, B., D. Collins, K. Braganza, D. Jakob, and D.A. Jones (2011). A high-quality monthly total cloud amount dataset for Australia. *Climatic Change*, 108, 485-517.
- Liu, M., A. Bárdossy, J. Li, and Y. Jiang (2012). GIS-based modelling of topography-induced solar radiation variability in complex terrain for data sparse region. *International Journal of Geographical Information Science*, 26(7), 1281-1308.
- Moore, I.D., T.W. Norton, and J.E. Williams (1993). Modelling environmental heterogeneity in forested landscapes. *Journal of Hydrology*, 150, 717-747.
- Ruiz-Arias, J.A., J. Tovar-Pescador, D. Pozo-Vázquez, and H. Alsamamra (2009). A comparative analysis of DEM-based models to estimate the solar radiation in mountainous terrain. *International Journal of Geographical Information Science*, 23(8), 1049-1076.
- Schaaf, C.B., F. Gao, A.H. Strahler and 19 others (2002) First operational BRDF, albedo nadir reflectance products from MODIS. *Remote Sensing of Environment*, 82, 135-148.
- Wilson, J.P. and J.C. Gallant (2000). Secondary topographic attributes, Chapter 4 in Wilson, J.P. and J.C. Gallant, *Terrain Analysis: Principles and Applications*. John Wiley and Sons, New York.